



Published in final edited form as:

*Cell Cycle*. 2010 April 15; 9(8): 1504–1510.

## Stem cell dynamics in mouse hair follicles:

### A story from cell division counting and single cell lineage tracing

Ying V. Zhang, Brian S. White, David I. Shalloway, and Tudorita Tumbar\*

Department of Molecular Biology and Genetics; Cornell University; Ithaca, NY USA

### Abstract

Understanding tissue stem cell behavior is a prerequisite for elucidating the mechanisms that govern their self-renewal and differentiation. Previously, we provided single cell lineage tracing and proliferation history data (based on H2B-GFP label dilution over time) in mouse hair follicles. We proposed a population deterministic model with symmetric stem cell fate decisions throughout life. Here we provide data suggesting that in hair follicle stem cells the self-renewing divisions within the niche (bulge) are symmetric with respect to localization of daughter cells near the basement membrane, an important niche component. In contrast, when cells migrate from the niche to the differentiating zone where they become short-lived progenitors, their daughter cells can adopt asymmetric orientation relative to the basement membrane. Furthermore, we document the dynamic re-localization of cells within the bulge to accommodate the hair follicle morphological changes through the hair cycle. In addition, we provide a method to compute the change in number of cells generated by division from H2B-GFP pulse-chase data, and to estimate the minimum cell loss encountered when the fold change can be experimentally determined. We computed a minimum of 42% of bulge cell loss during one hair cycle, a massive rate of loss previously unrecognized. Finally, we showed that a multipotent population of cells found at the junction zone between hair follicle and epidermis, known to express *Lrig1*, cycle more rapidly than some other hair follicle compartments.

### Keywords

hair follicle stem cells; population deterministic model; symmetric and asymmetric stem cell divisions; mathematical modeling of division data; H2B-GFP pulse-chase model

## Symmetric Daughter-Cell Fate Decisions for Infrequently Dividing Hair Follicle Stem Cells

Regenerative tissues contain stem cells (SCs) that self-renew and differentiate for an extended period of time. In normal tissue homeostasis SC division is thought to be infrequent and to involve an asymmetric daughter-cell-fate decision, in which one daughter remains a SC while the second partially differentiates into a progenitor cell with short-term growth potential.<sup>1–3</sup> This model was recently challenged by lineage tracing data in the undisturbed mouse epidermis, hair follicle and small intestine.<sup>4–6</sup>

In mouse skin, adult hair follicles undergo synchronous and periodic regeneration during the hair cycle, which consists of three morphologically distinct stages: quiescence (telogen), growth (anagen) and apoptotic regression (catagen).<sup>7</sup> The hair is composed of a temporary

differentiated region known as the bulb and a permanent un-differentiated region known as the bulge. The bulb contains progenitor matrix cells that differentiate into inner layers, including the hair shaft, and that undergo apoptosis during catagen. The bulge contains most of the hair follicle's infrequently dividing cells,<sup>8,9</sup> and its residents contribute to hair growth in transplantation assays.<sup>10-13</sup> The hair germ is thought to at least temporarily contain SCs,<sup>4,14</sup> and seems to arise from the bulge when its cells collapse around the hair club at the end of catagen.<sup>8</sup> Lineage tracing marking of bulge and germ cells also indicates that this region contains SCs.<sup>4,12</sup>

In a recent study we employed two experimental approaches to elucidate SC dynamics, the fate decision mechanism, and division rates in mouse hair follicles.<sup>15</sup> First, we used double transgenic K5tTA  $\times$  pTRE-H2B-GFP mice<sup>16</sup> to identify and trace H2B-GFP label retaining cells in the bulge and hair germ at distinct stages of tissue homeostasis. We found that upon feeding mice doxycycline (chase) to shut off H2B-GFP expression, the protein is diluted 2-fold following each division.<sup>16,17</sup> By a series of chase experiments across all stages of the first hair cycle and a combination of Fluorescence Activated Cell Sorting (FACS) and confocal microscopy, we quantified bulge cell proliferation at different stages and confirmed the infrequently dividing nature of both bulge and hair germ cells.<sup>15</sup> Moreover, we employed single bulge-cell lineage tracing using inducible K14CreER transgenic mice crossed with a Rosa26R reporter line.<sup>18</sup> Tamoxifen injection induces Cre recombinase to enter the nucleus where it initiates production of  $\beta$ -galactosidase (LacZ), which turns the cell blue upon X-gal staining.<sup>19</sup> We found that singly labeled bulge cells either leave their niche to differentiate and eventually die or stay in the niche to self-renew.<sup>15</sup> Collectively our findings are consistent with a population deterministic model that involves a symmetric daughter-cell-fate decision for bulge SC descendants. We proposed that, to avoid exhausting the small (1–2 cell) pool of SCs comprising a “simple” niche, as defined by Spradling et al.<sup>20</sup> a SC cannot leave it without first dividing to replenish and self-renew the remaining SC population (Fig. 1). A “storage” niche,<sup>20</sup> such as the hair follicle, is instead supported by large groups of clustered SCs, with residents behaving as a population in a manner similar to that proposed for the *C. elegans* germ line.<sup>1</sup> Individual SCs have equal potential to replenish the pool through division in the niche or to migrate away, proliferate, differentiate, and eventually die. Assignment to one of these two fates is likely dependent upon the distance of individual SCs from the signaling center (Fig. 1), which in the hair follicle is likely the dermal papilla (a mesenchymal structure at the base of the epithelial portion of the hair follicle).

Here we explore in more depth the nature of bulge cell division and the proliferation dynamics for a recently described multipotent cell population in the upper hair follicle.<sup>21</sup> Moreover, we provide a mathematical approach for estimating the expansion in number of bulge cells due to division based on H2B-GFP dilution data.

## Divisions with Respect to the Basement Membrane are Largely Asymmetric in the Hair Germ and Symmetric in the Bulge

Skin epithelial SCs are found among the basal layer cells, which express  $\alpha 6/\beta 4$  integrins and contact the basement membrane (BM),<sup>22</sup> a location important for SC maintenance.<sup>23</sup> When the mitotic spindle of a basal layer cell orients perpendicularly to the BM the distal daughter cell differentiates.<sup>24</sup> Here we examined the placement of two bulge or germ daughter cells with respect to the BM.

Previously, we found that in K14CreER  $\times$  Rosa26R mice 76% of labeled hair follicles had single cell labeling in a postnatal day (PD)17–21 chase.<sup>15</sup> Thus, we assume that most cell doublets found in the hair follicle at later stages are the two daughters descending from one

cell division. We analyzed 53 hair follicles at PD25 with doublets in the hair germ and found that ~41% of the doublets showed perpendicular orientation to the BM (Fig. 2A). Assuming hair follicle cells differentiate after losing contact with the BM, as in the epidermis,<sup>2,24</sup> we speculate that a bulge cell entering the hair germ can either divide symmetrically along the BM to expand the outer root sheath, or asymmetrically to produce a differentiating inner layer cell along with a renewed hair germ/matrix progenitor. We also analyzed 74 hair follicles containing X-Gal<sup>+</sup> doublets in the bulge at PD35 (during full anagen, following bulge cell division) and found ~81% of them parallel to the BM (Fig. 2B). These results suggest a strong bias for symmetric bulge cell division with respect to BM orientation of daughter cells (see Discussion).

### The Bias Towards Bulge-Cell Labeling is Cre Transgenic Line Dependent

Single cell lineage tracing is a powerful approach for studying SCs in vivo, but appropriate tools are lacking in most systems. Lineage tracing was possible in hair follicles because K14CreER labeling in our transgenic line occurs with low efficiency and, in telogen, is biased towards the bulge over the hair germ, despite the expected activity of the K14 promoter in both compartments and the demonstrated activity of the Rosa26 promoter in the hair germ of constitutively active K14Cre mice.<sup>18</sup> To test whether germ cells are less responsive to tamoxifen, we examined a second K14CreER mouse transgenic line (a gift from Dr. Pierre Chambon) referred to as K14CreERT2.<sup>25</sup> We found that in K14CreERT2 × Rosa26R mice, all skin epithelial compartments including the hair germ, were fully induced after 4 days (Fig. 3) throughout most of the skin. This suggests that the preference for bulge labeling is transgenic line dependent. We again found preferential bulge labeling in a third transgenic line, in which Cre is not driven by the K14 promoter and is expected to be expressed at low levels in the bulge and germ (unpublished data). We speculate that at low levels of Cre recombinase expression the bulge cells are more easily marked, possibly due to a more open chromatin structure in these cells relative to hair germ cells. Future studies on selected transgene insertions should facilitate single cell lineage tracing in other SC systems.

### Proliferation Dynamics at the Hair Follicle Junctional Zone Reveals Higher Activity when Compared to the Bulge

Using the H2B-GFP inducible expression system, we previously quantified the proliferation history of a CD34<sup>+</sup>/α6-integrin<sup>+</sup> bulge cell population by flow cytometry, and of single bulge and germ cells in situ by confocal optical sectioning of thick skin sections.<sup>15,17</sup> These data confirmed the slow cycling nature of bulge and hair germ cells, most of which divided 2–5 times in one hair cycle. Insofar as infrequent division is a “stemness” marker, it is of interest to relate bulge proliferation to that of other multipotent cell populations, such as that expressing Leucine-rich repeats and immunoglobulin-like domain protein 1 (Lrig1) at the hair follicle junctional zone adjacent to the sebaceous gland and infundibulum.<sup>21</sup> Lrig1<sup>+</sup> cells can give rise to all of the epidermal lineages, including the hair follicle, upon transplantation.<sup>21</sup> To quantify the proliferation of this newly characterized population, we applied the single cell division counting method to hair follicle junctional zone cells through the first adult hair cycle.

We fed the tet-off H2B-GFP expression mice doxycycline starting at telogen (PD21), and collected tissue at early anagen (PD28), full anagen (PD35) and the telogen of the next hair cycle (PD44). Thick cryo-sections of skin (100 μm) were stained with TOPRO3 DNA dye and imaged by confocal optical sectioning (reviewed in ref. 15). We found that cells at the junctional zone in general possessed less H2B-GFP than bulge cells, suggesting more vigorous proliferation activity (Fig. 4A). Next, we summed the H2B-GFP fluorescent intensity at each sectioning plane to calculate the total volume intensity of randomly selected

cells. From PD21 to PD28, bulge cells divided 0–3 times, whereas cells in the junctional zone divided 3–5 times (Fig. 4B). By full anagen at PD35, we showed previously that bulge cells divided 1–5 times.<sup>15</sup> Here we find that most cells in the junctional zone divided 5 or more times by PD35 with rare incidence of 4 divisions (Fig. 4B). At the next telogen (PD44), the proliferation profile of junctional zone cells remained similar to that of PD35, suggesting a quiescent stage around catagen, in line with Ki67 and short term BrdU labeling (not shown). This pause in proliferation coincides with the limited proliferation in the bulge and hair germ at the same stage (Fig. 4B, reviewed in ref. 15). Thus, we conclude that cells in the junctional zone proliferate nearly twice as much as bulge and hair germ cells. The slow-cycling cells identified by DNA label retention in the junctional zone<sup>26</sup> are probably the few we identified that divide 4–5 times in one hair cycle.

## Lateral Migration of Bulge Cells in Catagen in the Newly Generated Club Hair Re-Creates the Niche

The fraction of CD34<sup>+</sup>/α6-integrin<sup>+</sup> in the skin detected by flow cytometry, although variable, appears to increase from first to second telogen, which is in line with bulge cell divisions in >90% of bulge cells within this hair cycle.<sup>15,17,27</sup> Since CD34<sup>+</sup>/α6-integrin<sup>+</sup> bulge cells cluster around the old club hair site (old bulge site) during first telogen but are found in the new club site (new bulge site) by second telogen,<sup>13</sup> it seems possible that these cells migrate laterally during catagen, when non-bulge outer root sheath cells found at the (future) new bulge site undergo apoptosis. To test the hypothesis that cells re-localize to the new bulge site, we used confocal microscopy to track the brightest H2B-GFP bulge cells during one hair cycle in sum projections through the z (longitudinal view) and y (cross-sectional) axes. We found trails of bright cells emanating from the old bulge site towards the new bulge site by PD35, and a re-localization of some of the bright cells in the new club hair site and into the hair germ by PD44 (late catagen/telogen) (Fig. 4C). These lateral movements are likely driven first by apoptosis of non-bulge cells at the new bulge site, and second by overcrowding of cells at the old bulge site.

## Quantification of H2B-GFP Pulse-Chase Data Provides a Model-Independent Measure of Cell-Population Size Increase and of Minimum Cell Loss

An important indicator of tissue dynamics and growth is the fold change ( $fc$ ) in its population size between an initial time  $t_0$  and a final time  $t_1$ , e.g., the number of cells  $N_1^b$  found in the bulge at  $t_1$  relative to the number of initial bulge cells  $N_0^b$  at  $t_0$ :

$$fc = \frac{N_1^b}{N_0^b}.$$

Here we provide a method for calculating the fold change due to division based on H2B-GFP chase FACS data, and, in particular, on the fraction  $p_{t_0 \rightarrow t_1, n}$  ( $n \geq 0$ ) of H2B-GFP-labeled cells that have divided  $n$  times and that are derived from the corresponding peaks of the FACS histograms of CD34<sup>+</sup>/α6-integrin<sup>+</sup> bulge cells at the end of the chase ( $t_1$ ) (Supplement). Significantly, the calculation makes assumptions neither about the mechanism of bulge replication (e.g., it is independent of the proliferative history that lead to the  $p_{t_0 \rightarrow t_1, n}$ ) nor about the absolute number of cells within the population of interest. The key assumption is that the total H2B-GFP content (summed across all labeled bulge cells)

decays due to protein degradation,<sup>17</sup> but does not depend on the number of replications since H2B-GFP is distributed, while being conserved, between cells at division.

The  $fc$  calculation balances total H2B-GFP content at  $t_1$  under two situations: a hypothetical one in which none of the initial  $N_0^b$  bulge divide and an experimentally-realized situation yielding  $N_1^{tot}$  cells at  $t_1$  that are the progeny of the original cells.  $N_1^b$  of these remain in the bulge and  $N_1^l$  are lost from the bulge (e.g., due to apoptosis, export to the hair germ, or other down-regulation of bulge markers), so that  $N_1^{tot} = N_1^b + N_1^l$ .

Consider the H2B-GFP content of the cells in each histogram peak at  $t_1$ : The fraction  $p_{t_0 \rightarrow t_1, 0}$  of cells in the  $n = 0$  division peak constitute  $N_1^b \cdot p_{t_0 \rightarrow t_1, 0}$  cells, each with a fluorescence of 1 (in arbitrary dimensionless units), for a total contribution of  $N_1^b \cdot p_{t_0 \rightarrow t_1, 0} \cdot 1$ . Owing to the 2-fold dilution following division, each of the  $N_1^b \cdot p_{t_0 \rightarrow t_1, 1}$  cells in the  $n = 1$  peak have fluorescence  $1/2$ , for an aggregate contribution of  $N_1^b \cdot p_{t_0 \rightarrow t_1, 1} \cdot \frac{1}{2}$ . By extension, each of the  $N_1^b \cdot p_{t_0 \rightarrow t_1, n}$  cells in peak  $n$  have fluorescence  $\left(\frac{1}{2}\right)^n$ , for an aggregate contribution of  $N_1^b \cdot p_{t_0 \rightarrow t_1, n} \cdot \left(\frac{1}{2}\right)^n$ . Summing these contributions across peaks gives the total H2B-GFP content in the bulge at the end of chase ( $t_1$ ):

$$N_1^b \cdot p_{t_0 \rightarrow t_1, 0} \cdot 1 + N_1^b \cdot p_{t_0 \rightarrow t_1, 1} \cdot \frac{1}{2} + N_1^b \cdot p_{t_0 \rightarrow t_1, 2} \cdot \left(\frac{1}{2}\right)^2 + \dots = N_1^b \cdot \sum p_{t_0 \rightarrow t_1, n} \cdot \left(\frac{1}{2}\right)^n.$$

By a similar argument, the total H2B-GFP content lost from the bulge by  $t_1$ , defined in terms of the (unknown) probabilities  $p_{t_0 \rightarrow t_1, n}^l$  that a lost cell has divided  $n$  times, is

$N_1^l \cdot \sum p_{t_0 \rightarrow t_1, n}^l \cdot \left(\frac{1}{2}\right)^n$ . The sum of the H2B-GFP content across all  $N_1^{tot}$  cells must equal the total fluorescence  $N_0^b \cdot 1$  in the bulge had the bulge cells not divided at all, which implies

$$N_0^b \cdot 1 = N_1^b \cdot \sum p_{t_0 \rightarrow t_1, n} \cdot \left(\frac{1}{2}\right)^n + N_1^l \cdot \sum p_{t_0 \rightarrow t_1, n}^l \cdot \left(\frac{1}{2}\right)^n. \tag{1}$$

and, after rearranging,

$$fc = \frac{N_1^b}{N_0^b} = \frac{1 - (N_1^l/N_0^b) \cdot \sum_n p_{t_0 \rightarrow t_1, n}^l \cdot \left(\frac{1}{2}\right)^n}{\sum_n p_{t_0 \rightarrow t_1, n} \cdot \left(\frac{1}{2}\right)^n}. \tag{2}$$

$$fc_{no\ loss} = \frac{1}{\sum_n p_{t_0 \rightarrow t_1, n} \cdot \left(\frac{1}{2}\right)^n} > \frac{1 - (N_1^l/N_0^b) \sum_n p_{t_0 \rightarrow t_1, n}^l \cdot \left(\frac{1}{2}\right)^n}{\sum_n p_{t_0 \rightarrow t_1, n} \cdot \left(\frac{1}{2}\right)^n} = fc \tag{3}$$

Although applying Eq. (2) may be impractical since it depends on unknown parameters for cell loss  $p_{t_0 \rightarrow t_1, n}^l$  that would be challenging to determine experimentally, it may be bounded by  $fc_{no\ loss}$ , the fold change calculated under the hypothesis of no cell loss (i.e., with  $N_1^l = 0$ ).

The inequality holds because of the non-negativity of the second term in the numerator.

$fc_{no\ loss}$  can be calculated from H2B-GFP division data peaks (Fig. 1E in ref. 15) to bound tissue expansion across different postnatal periods (Fig. 5). For example, the number of bulge cells increases by an  $fc_{no\ loss}^{PD22-25}$  of  $\sim 1.9$  in the first 3 days of chase and an  $fc_{no\ loss}^{PD21-28}$  of  $\sim 2.7$  across a seven day chase in early anagen. The results assume that any small fraction of bulge cells with H2B-GFP fluorescence below the detection limit (i.e., a “dim” peak) is comprised entirely of cells unlabeled due to mosaicism.<sup>17</sup> The dim peak might also contain highly proliferative cells with diluted H2B-GFP fluorescence indistinguishable from that of unlabeled cells. A more conservative calculation accounts for such highly proliferative cells and shows that our assumption leads to a slight underestimation of  $fc$ , though the underestimation of average number of divisions (also shown in Fig. 5) may be more extreme (Supplement).

To characterize the growth during anagen we calculated an  $fc_{no\ loss}^{PD21-35}$  of  $\sim 3.4$ . However, when we counted the number of cells in the outer layer of the bulge, as defined morphologically in 20  $\mu\text{m}$  skin sections at the first and second telogen, we found an  $\sim 2$ -fold increase. This was likely due to the generation during the interval of a second club hair present in the bulge area. This gross discrepancy between the calculated and expected results led us to reject the hypothesis of no cell loss. However, we can rearrange Eq. (2) and use it to establish a minimum bound on the ratio of cells lost to those initially in the bulge  $N_1^l/N_0^b$  (Supplement)

$$\frac{N_1^l}{N_0^b} \geq 1 - (N_1^b/N_0^b) \cdot \sum_n p_{t_0 \rightarrow t_1, n} \cdot \left(\frac{1}{2}\right)^n. \quad (4)$$

Substituting the expected fold change between PD21 and PD35,  $N_1^b/N_0^b = 2$ , allows us to estimate the minimum fractional cell loss:  $N_1^l/N_0^b > 0.42$ . Assuming that the fractional cell loss, derived from the many bulges analyzed in a skin sample, is indicative of an individual bulge, we may multiply it by the  $\sim 150$  cells expected to constitute a single bulge at PD21 (Supplement) to determine that more than  $\sim 63$  bulge cells must be lost in one hair cycle.

## Conclusions

Here we provided a detailed analysis of the dynamics of tissue growth and of cell fate decisions in the hair follicle. Using our H2B-GFP division counting tools in situ we characterized the proliferation activity of a newly-identified multipotent cell population in the hair follicle junctional zone,<sup>21</sup> and found that these cells cycle more actively than bulge cells. These data should be useful in future experiments aimed at characterizing the role of this population in the skin and hair follicle.

Second, we analyzed the placement of two daughter cells descending from one cell division with respect to an important component of the stem cell niche, the basement membrane. Our data suggest that when a bulge cell moves into the differentiation zone—the hair germ—it either divides symmetrically along the BM to expand the hair germ/outer root sheath pool, or asymmetrically likely to simultaneously produce a differentiating inner layer and a



renewed progenitor/matrix cell contacting the BM. However, although these matrix precursor cells divide asymmetrically they do not fulfill the accepted definition of a stem cell, since they fail to self-renew after a short period of activity, as shown by lineage tracing data,<sup>15,28</sup> and instead best qualify as transit-amplifying or progenitor cells. In contrast, the permanent cells of the bulge divide symmetrically with respect to the basement membrane during anagen. This was predicted by our model (Fig. 1), in which loss of SCs from the pool by downward movement is compensated by symmetric SC expansion in the niche to replenish the pool throughout life. It is important to note that orientation with respect to the BM is only one aspect of asymmetric cell division and additional components of the fate determinant cellular distribution machinery should be explored in the future. Our attempt to examine the distribution of Numb (antibody a gift from Dr. W. Zhang (Yale U.)) and Par3 (antibody a gift from Dr. I. Macara (U. Virginia)) revealed ubiquitous distribution in interphase, and did not provide reliable signal in mitosis (as defined by phospho H3 staining) with our current methods.

Our previous model (ref. 15, and Fig. 1) implicates symmetric fate decision for bulge cell daughters without reference to the symmetric or asymmetric nature of the bulge cell division itself. In principle, cells that result from an asymmetric division might still adopt symmetric fates given a system sufficiently robust and flexible to adopt influences from the environment or given reversible differentiation cellular states. A simple interpretation of the data presented here predicts that in a relatively long-lived animal, such as the mouse, the progenitor cells divide asymmetrically for defined periods of time during which they actively sustain tissue growth, while the true long-lived stem cells behave as a reservoir that periodically sacrifices a fraction of its residents to be expelled from the niche, become progenitors, differentiate, and eventually die. The SC pool would be replenished by symmetric expansion subsequent to loss due to active migration or passive downward movement. This two-gear system would permit the stem cells to remain relatively infrequently dividing over long-periods of time to reduce the rate of cancer, a challenge that a short-lived animal would not have to encounter. In other words, the progenitor cells in a mouse might behave as stem cells in a short-lived animal such as *Drosophila*.

Previously we noted that the amount of proliferation detected in the bulge during one hair cycle is incompatible with a previously adopted model in which only little bulge cellular turnover might take place in one hair cycle.<sup>17</sup> The extent of bulge-cell proliferation suggested that more cellular export from the bulge into the bulb must occur than previously recognized,<sup>28</sup> or else a significant fraction of bulge cells generated in anagen must die. Here we provided an approach for calculating an upper bound on the expansion of a cell population (fold change) based of H2B-GFP pulse chase data, which is insensitive to a particular replication model, for future use by the Developmental Biology community. When the actual number of cells can be experimentally determined, this upper bound can be used to estimate the minimum amount of cell loss, a measure that cannot be easily derived from experimental data. Our calculations indicated massive (42%) bulge cell loss in one hair cycle. We are currently in the process of modeling the number of cells exported from the bulge to contribute to bulb.

According to our H2B-GFP chases, proliferation occurs continuously during anagen (up to PD35) in a majority of the bulge cells and results in near doubling in the number of bulge cells by the end of the first hair cycle. Intriguingly, these cells remain confined around the old club hair site until early catagen, as suggested by lack of re-distribution in X-Gal labeling among hair follicles from PD25–35 (Fig. 4 in ref. 15) and by CD34 staining (data not shown). Therefore it is tempting to speculate that upon division in anagen an increase in bulge cell density could lead to contact inhibition which would eventually result in cessation of proliferation.<sup>29</sup> Over-crowding of bulge cells around the old club hair site might therefore

force the cells to re-organize and spread into adjacent areas towards the new club hair site to relieve the presumed contact inhibition. This hypothesis is in line with our detection of lateral movements in the H2B-GFP label retaining bulge cells from the old club hair towards the newly generated club hair in catagen (Fig. 4). This step might be necessary to prepare the niche for a new cycle of proliferation and expansion in the next anagen. The control of stem cell pool size by a feed-back inhibition loop due to cell-cell contact is an area of future exploration.

## Supplementary Material

Refer to Web version on PubMed Central for supplementary material.

## Acknowledgments

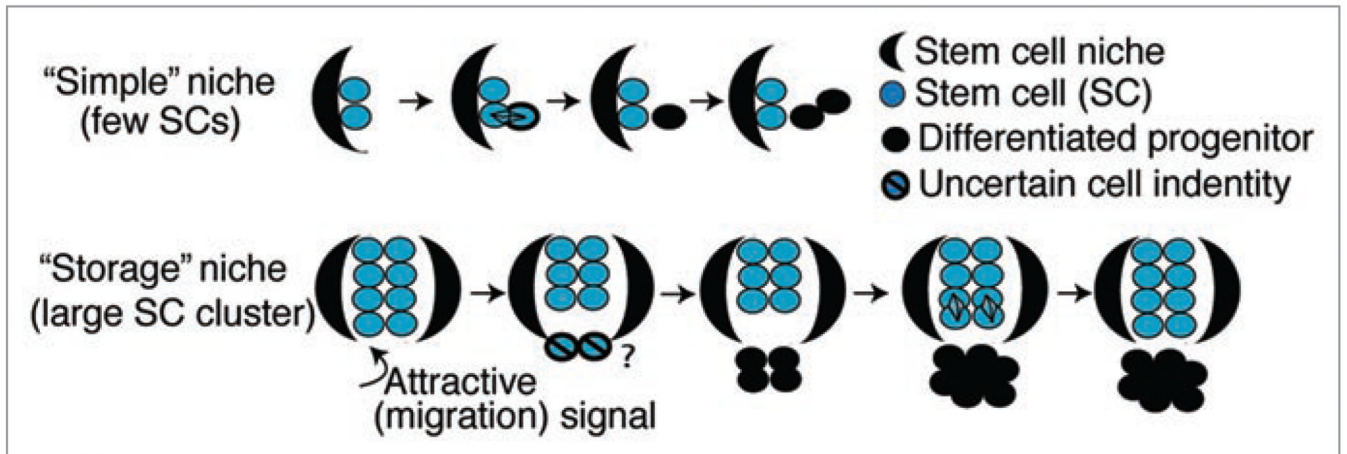
Funding was from NIH/NIAMS AR053201 and from NYSTEM C024354 grants to T.T.

## References

- Morrison SJ, Kimble J. Asymmetric and symmetric stem-cell divisions in development and cancer. *Nature*. 2006; 441:1068–1074. [PubMed: 16810241]
- Fuchs E. The tortoise and the hair: slow-cycling cells in the stem cell race. *Cell*. 2009; 137:811–819. [PubMed: 19490891]
- Dor Y, Melton DA. How important are adult stem cells for tissue maintenance? *Cell Cycle*. 2004; 3:1104–1106. [PubMed: 15326371]
- Jaks V, Barker N, Kasper M, van Es JH, Snippert HJ, Clevers H, et al. Lgr5 marks cycling, yet long-lived, hair follicle stem cells. *Nat Genet*. 2008; 40:1291–1299. [PubMed: 18849992]
- Barker N, van Es JH, Kuipers J, Kujala P, van den Born M, Cozijnsen M, et al. Identification of stem cells in small intestine and colon by marker gene Lgr5. *Nature*. 2007; 449:1003–1007. [PubMed: 17934449]
- Clayton E, Doupe DP, Klein AM, Winton DJ, Simons BD, Jones PH. A single type of progenitor cell maintains normal epidermis. *Nature*. 2007; 446:185–189. [PubMed: 17330052]
- Cotsarelis G. Epithelial stem cells: a folliculocentric view. *J Invest Dermatol*. 2006; 126:1459–1468. [PubMed: 16778814]
- Ito M, Kizawa K, Hamada K, Cotsarelis G. Hair follicle stem cells in the lower bulge form the secondary germ, a biochemically distinct but functionally equivalent progenitor cell population, at the termination of catagen. *Differentiation*. 2004; 72:548–557. [PubMed: 15617565]
- Taylor G, Lehrer MS, Jensen PJ, Sun TT, Lavker RM. Involvement of follicular stem cells in forming not only the follicle but also the epidermis. *Cell*. 2000; 102:451–461. [PubMed: 10966107]
- Hoffman RM. The pluripotency of hair follicle stem cells. *Cell Cycle*. 2006; 5:232–233. [PubMed: 16410728]
- Claudinot S, Nicolas M, Oshima H, Rochat A, Barrandon Y. Long-term renewal of hair follicles from clonogenic multipotent stem cells. *Proc Natl Acad Sci USA*. 2005; 102:14677–14682. [PubMed: 16203973]
- Morris RJ, Liu Y, Marles L, Yang Z, Trempus C, Li S, et al. Capturing and profiling adult hair follicle stem cells. *Nat Biotechnol*. 2004; 22:411–417. [PubMed: 15024388]
- Blanpain C, Lowry WE, Geoghegan A, Polak L, Fuchs E. Self-renewal, multipotency and the existence of two cell populations within an epithelial stem cell niche. *Cell*. 2004; 118:635–648. [PubMed: 15339667]
- Greco V, Chen T, Rendl M, Schober M, Pasolli HA, Stokes N, et al. A two-step mechanism for stem cell activation during hair regeneration. *Cell Stem Cell*. 2009; 4:155–169. [PubMed: 19200804]
- Zhang YV, Cheong J, Ciapurin N, McDermitt DJ, Tumber T. Distinct self-renewal and differentiation phases in the niche of infrequently dividing hair follicle stem cells. *Cell Stem Cell*. 2009; 5:267–278. [PubMed: 19664980]



16. Tumber T, Guasch G, Greco V, Blanpain C, Lowry WE, Rendl M, et al. Defining the epithelial stem cell niche in skin. *Science*. 2004; 303:359–363. [PubMed: 14671312]
17. Waghmare SK, Bansal R, Lee J, Zhang YV, Mc Dermitt DJ, Tumber T. Quantitative proliferation dynamics and random chromosome segregation of hair follicle stem cells. *EMBO J*. 2008; 27:1309–1320. [PubMed: 18401343]
18. Vasioukhin V, Degenstein L, Wise B, Fuchs E. The magical touch: genome targeting in epidermal stem cells induced by tamoxifen application to mouse skin. *Proc Natl Acad Sci USA*. 1999; 96:8551–8556. [PubMed: 10411913]
19. Soriano P. Generalized lacZ expression with the ROSA26 Cre reporter strain. *Nat Genet*. 1999; 21:70–71. [PubMed: 9916792]
20. Spradling A, Drummond-Barbosa D, Kai T. Stem cells find their niche. *Nature*. 2001; 414:98–104. [PubMed: 11689954]
21. Jensen KB, Collins CA, Nascimento E, Tan DW, Frye M, Itami S, et al. Lrig1 expression defines a distinct multipotent stem cell population in mammalian epidermis. *Cell Stem Cell*. 2009; 4:427–439. [PubMed: 19427292]
22. Fuchs E, Raghavan S. Getting under the skin of epidermal morphogenesis. *Nat Rev Genet*. 2002; 3:199–209. [PubMed: 11972157]
23. Hynes RO. The extracellular matrix: not just pretty fibrils. *Science*. 2009; 326:1216–1219. [PubMed: 19965464]
24. Lechler T, Fuchs E. Asymmetric cell divisions promote stratification and differentiation of mammalian skin. *Nature*. 2005; 437:275–280. [PubMed: 16094321]
25. Li M, Indra AK, Warot X, Brocard J, Messaddeq N, Kato S, et al. Skin abnormalities generated by temporally controlled RXRalpha mutations in mouse epidermis. *Nature*. 2000; 407:633–636. [PubMed: 11034212]
26. Braun KM, Niemann C, Jensen UB, Sundberg JP, Silva-Vargas V, Watt FM. Manipulation of stem cell proliferation and lineage commitment: visualisation of label-retaining cells in whole mounts of mouse epidermis. *Development*. 2003; 130:5241–5255. [PubMed: 12954714]
27. Osorio KM, Lee SE, Mc Dermitt DJ, Waghmare SK, Zhang YV, Woo HN, et al. Runx1 modulates developmental, but not injury-driven, hair follicle stem cell activation. *Development*. 2008; 135:1059–1068. [PubMed: 18256199]
28. Legue E, Nicolas JF. Hair follicle renewal: organization of stem cells in the matrix and the role of stereotyped lineages and behaviors. *Development*. 2005; 132:4143–4154. [PubMed: 16107474]
29. Lien WH, Klezovitch O, Vasioukhin V. Cadherincatenin proteins in vertebrate development. *Curr Opin Cell Biol*. 2006; 18:499–506. [PubMed: 16859905]

**Figure 1.**

Stem cell niche models. In “simple” niches stem cells divide asymmetrically to make one stem cell daughter and a committed progenitor daughter. In “storage” niches stem cells near the niche boundary respond to the attractive signal by migrating out of the niche and subsequently differentiating. Remaining stem cells divide symmetrically to replenish the stem cell pool.

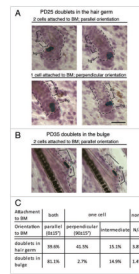


**Figure 2.**

Placement of two bulge daughter cells with respect to the niche. Skin sections (20  $\mu\text{m}$ ) from K14CreER  $\times$  Rosa26R mice (injected with tamoxifen at PD17 and stained for X-Gal and hematoxylin at days indicated) show doublet orientation with respect to the basement membrane (BM) and in two distinct compartments: the differentiating zone (hair germ) and the stem cell niche (bulge). (A) Bulge cells exported in the germ divided both parallel (top) and perpendicular (bottom) with respect to the BM. (B) Bulge cells that continue to reside in the niche divided parallel to the BM. (C) Quantification of data in (A and B). BM, black dotted lines; Bu, bulge; hg, hair germ. Scale bar, 50  $\mu\text{m}$ . N = 127 hair follicles.

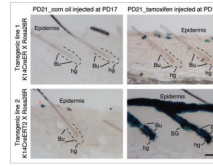


**Figure 3.**

Distinct transgene activation in two K14CreER mouse lines. Skin sections (60  $\mu\text{m}$ ) from two mouse lines (as indicated at the left of the panel) injected with tamoxifen (100  $\mu\text{g/g}$  body) or corn oil (carrier) at PD17 and sacrificed at PD21 were stained for X-Gal (blue). Note single-cell bulge labeling in hair follicles from the K14-CreER line with no leaky expression in the absence of tamoxifen (top). In contrast, the K14CreERT 2 line showed robust induction in all hair compartment including hair germ, as well as some leaky expression (bottom). Basement membrane around the bulge and hair germ marked with dotted lines. Bu, bulge; hg, hair germ; SG, sebaceous gland. Scale bar, 50  $\mu\text{m}$ . N = 3 mice per transgenic line.

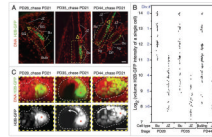


**Figure 4.**

Proliferation at the junctional zone and lateral movement of bulge cells in catagen. (A) A single optical confocal slice from image stacks illustrates H2B-GFP retention in the bulge (Bu) as compared to the junctional zone (JZ) after each experiment. (B) Quantification of volume H2B-GFP intensity by integration through the optical stack for individual cells located in different hair follicle compartments defined by morphology. Cell divisions numbers were assigned to cells based on 2-fold dilution of H2B-GFP intensity per division, and the estimate that the brightest cells did not divide (reviewed in ref. 17). (C) Top view sum projection of the bulge region stacks highlighted in (A) with yellow dotted box revealing active re-localization of bright H2B-GFP cells from the old club hair shaft (red asterisks) to the new bulge region (indicated by white arrow). hg, hair germ; SG, sebaceous gland; DP, dermal papilla. All skin sections were 100  $\mu\text{m}$  thick and stained with TOPRO3 DNA dye. Scale bars, 20  $\mu\text{m}$ . N = 10 hair follicles per stage.

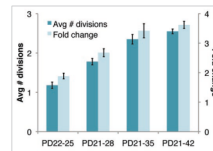


**Figure 5.**

Average number of divisions and bulge population size fold change based on H2B-GFP-division tracking data calculated at indicated time periods assuming H2B-GFP cells with fluorescence below the background are unlabelled due to mosaicism. This provides an underestimate for average divisions but not for the fold change (Supplement). Error bars are 90% credible sets.